energies

MDPI

Review

A Review on the Preliminary Design of Axial and Radial Turbines for Small-Scale Organic Rankine Cycle

Enhua Wang * and Ningjian Peng

School of Mechanical Engineering, Beijing Institute of Technology, Beijing 100081, China
* Correspondence: wangenhua@bit.edu.cn

Abstract: Organic Rankine cycle (ORC) is an effective technology to harness low-grade energy. Turbine, as a key component of ORC, takes advantages of its high efficiency and compact size compared with other expanders. Currently, developing suitable turbines with a high performance and a low cost is one of the bottlenecks for wide applications of various ORCs. In this context, technical progress on radial inflow turbines (RITs), axial turbines (ATs), and radial outflow turbines (ROTs) is introduced, and loss models used in the preliminary design are compared, especially for small-scale ORCs. RIT is recommended for medium and small ORCs with an expansion pressure ratio of <10. The power outs and rotational speeds of the designed RITs spanned the ranges of 9.3–684 kW and 3000–114,000 r/min with an efficiency of 56.1–91.75%. In comparison, the power outputs and speeds of ATs were 3–2446 kW and 3000–91,800 r/min with an efficiency of 63–89.1%. AT is suitable for large-scale ORCs with a power output of greater than hundreds of kW. However, AT with impulse stages is feasible for small-scale ORCs when the pressure ratio is high, and the mass flow rate is small. The power outputs of the designed ROTs were relatively small, at 10–400 kW with a speed of 7200–42,700 r/min and an efficiency of 68.7–85%. For organic working fluids with a large expansion pressure ratio, ROT might be employed. Conventional mean-line models may neglect the effects of supersonic flow, which will be encountered in many ORC turbines. Therefore, adequate models for supersonic expansion loss and shock loss need to be added. Meanwhile, a proper multivariable optimization algorithm such as a gradient-based or stochastic search method should be selected. Finally, the challenges and potential research directions are discussed. The outcomes can provide some insights for the development of ORC turbines and the optimization of ORC systems.

Keywords: organic Rankine cycle; axial turbine; radial turbine; preliminary design; mean-line model

Citation: Wang, E.; Peng, N. A Review on the Preliminary Design of Axial and Radial Turbines for Small-Scale Organic Rankine Cycle. *Energies* **2023**, *16*, 3423. https://doi.org/10.3390/en16083423

Academic Editor: Antonio Calvo Hernández

Received: 7 February 2023
Revised: 4 April 2023
Accepted: 10 April 2023
Published: 13 April 2023

1. Introduction

Organic Rankine cycle (ORC) is an effective approach for energy conservation and low-grade energy utilization [1], which can be used in power generation from solar [2] and geothermal [3] energy, waste heat recovery [4] from power systems [5] and other industrial plants [6]. Meanwhile, ORC can be integrated with fuel cells to improve clean hydrogen energy utilization [7]. Currently, high-performance expander development is one of the bottlenecks for various applications of ORCs.

Positive displacement expanders, such as scroll expanders and piston expanders, are widely investigated for ORC systems [8]. Turbines are another promising option. Compared with positive displacement expanders, turbines have the advantages of high pressure ratio, high efficiency, large volumetric power density, and compact size [9]. Alshammari et al. [10] compared the performance characteristics of turbines and positive displacement expanders. Quoilin et al. [11] compared three maps for radial inflow turbines (RIT), screw expanders, and scroll expanders under feasible operation conditions when the power of ORC varied from kW to MW with the heat source temperature of 90–300 °C. For a specified operation condition, the most appropriate expander could be selected from the maps. Colonna et al. [12] analyzed the current status and future developing trend of turbines and positive

displacement expanders. In practice, noise, sealing, durability, leakage, and the feasibility of operating with wet vapor also need to be considered [13]. For small-scale expanders, experimental results indicated that the efficiency of a scroll expander was in the range of 60–70%, while it was 65–85% for the RIT [14]. Qyyum et al. [15] deemed that turbines were suitable for a power output up to 20 kW. Screw expanders were better when the power output was slightly higher. The performances of turbines and positive displacement expanders were similar for the power range of 20–70 kW.

Organic working fluids, instead of steam, are often employed in ORCs, which may experience an expansion process with a high volumetric expansion ratio and a low enthalpy drop. RITs exhibit a higher efficiency compared with other expanders for many ORCs. An efficiency of 85% might be achieved for RITs [16]. In comparison, an axial turbine (AT) is suitable for ORCs with a high mass flow rate. The efficiency of AT is comparable with RIT for some large-scale ORCs [17]. The diameters at the inlet and exit are different for RIT, which could increase the power output with a compact size and a low cost. Hence, RITs are superior for ORCs with a relatively high pressure ratio and a low mass flow rate. Zywica et al. [18] found that the efficiency of RIT was greater than AT when the power output ranged from several to tens of kW. For turbines with a power of 3–100 kW, Weib [19] pointed out that a single-stage axial impulse turbine might be the best for the integrated design of turbine-generator. In practice, a suitable expander must be designed according to the requirements of ORC, and a comprehensive performance estimation over the design and off-design conditions must be conducted.

Turbines as a critical component have been investigated from small-scale kW-class to large-scale MW-class ORC systems. Recently, rapid progress had been made in the design of turbines for ORCs. The preliminary design is fundamental for the development of a turbine with high efficiency. The applications of ORCs are diverse. The operation conditions and working fluid differ from one another. The preliminary design can be employed to determine the principle geometric parameters: rotational speed, power output, and turbine efficiency. Meanwhile, it can be integrated with the ORC model to give a more accurate estimation of system performance. In ORCs, RIT, AT, and radial outflow turbine (ROT) have been developed. The loss model is critical for the preliminary design. Meanwhile, several decision variables need to be optimized simultaneously, and an efficient optimization algorithm is important as well. However, there is a lack of an outline of these achievements. Therefore, in this context, the technical progress of three typical turbines, including RIT, AT, and ROT, is introduced, and the corresponding preliminary design approaches are presented. The loss models used in the mean-line method are analyzed and summarized. Subsequently, multivariable optimization algorithms used in the preliminary design process are reviewed. The outcomes can provide a reference for the development of high-performance turbines for ORCs.

2. Turbine Performance

The mean-line model is employed ordinarily for the preliminary design of turbine. The main geometric parameters of the stator and rotor are determined. The turbine performances under design and off-design conditions can be estimated. A typical procedure for the preliminary design is shown in Figure 1. In the initialization step, the working conditions of the turbine are configured according to the requirements of ORC. Normally, the total pressure and temperature at the turbine inlet, the static pressure at the exit, and the mass flow rate of the organic working fluid are given. A set of decision variables is defined with initial values, and the associated constraints for the optimization model are setup. Subsequently, an iterative computation process is built to optimize the target. The velocity triangles of the stator are determined according to the assumed values of the geometry. The flow losses are estimated accordingly based on the mean-line model. Then, the velocity triangles of the rotor are determined, and the losses are calculated in a similar manner. Hence, the efficiency and principle geometric parameters of the turbine are obtained. A multivariable optimization algorithm is often integrated to maximize the turbine efficiency.

The algorithm searches in the defined constraint space of the decision variables to optimize the target via an iterative computation. Once the convergence condition is satisfied, the iteration terminates, and the last results are stored. In this review, only the results about the preliminary design of ORC turbines based on the mean-line method are introduced. Some state-of-the-art investigations about CFD simulation, turbine experiments, and combined optimization with ORCs are not involved.

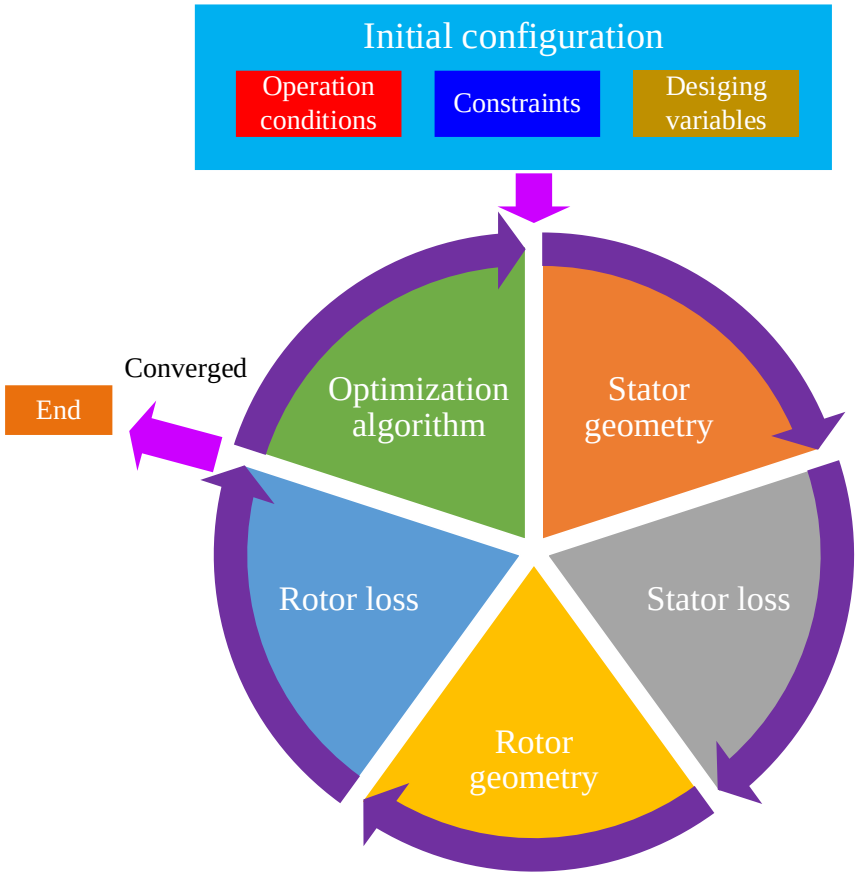

Figure 1. Procedure for the preliminary design of ORC turbines.

2.1. Radial Inflow Turbine

The performances of RITs were investigated widely for small-scale ORCs. Compared with AT, the flow of the working fluid inside RIT yields a decrease in radial radius. Thus, more work can be generated, and high efficiency is achieved. Table 1 lists the performances of various RITs designed for ORCs. It can be seen that the power outputs were in the range of 9.3–684.26 kW. Most of the RITs had an efficiency of over 80%. The maximum efficiency arrived at 91.75%. Different working fluids were employed, including refrigerants (R245fa, R1234yf, R143a, R152a), hydrocarbons (toluene, propane, isobutane), and siloxanes (D_4, MM). The designed turbine speed ranged from 3000 to 114,000 r/min, which might be apparently lower than that of a small-scale gas turbine [20]. The expansion pressure ratios (EPRs) were in the range of 1.997–7.95 for most turbines. A high EPR was specified for working fluids with a large molecular weight, such as toluene, MM, and D_4, which were 25, 72.3, and 49.43, respectively, because of a very low condensation pressure under the ambient temperature for these organic working fluids.

Table 1. Performances of the RITs investigated in the literature.

Working Fluid	EPR	Speed (r/min)	Power (kW)	Efficiency (%)	Refs.
R245fa	4.11	22,529	100	89.23	[21]
Novec 649	7	40,000	13.6	74.4	[22]
Toluene	25	71,502	45.6	56.1	[23]
Isobutane	4.491	49,331	105.08	76.36	[24]
R152a	1.997	43,124	15	84	[25]
R245fa	7.95	8995	684.26	86.9	[26]
R1234yf	3.638	30,673	50.2	78	[27]
R245fa	2.96	7000	293.9	87.3	[28]
R143a	2.54	24,250	414.83	81.72	[29]
D_4	49.43	25,990	9.6	78	[30]
MM	25	114,000	9.3	80	[31]
MM	72.3	90,200	11.6	77.3	[32]
R1234yf	4.4786	18,837	182	86.1	[33]
Propane	4.86	57,579	140	84.1	[34]
R245fa	2.69	11,000	128	87.23	[35]
R141b	3.17	3000	268	91.75	[36]

The preliminary design is the first step in the development of RITs and is generally realized based on the mean-line model. Jung et al. [28] designed a turbine with a net power output of 250 kW using R245fa as the working fluid. At the design condition, the turbine efficiency was 87.3% at a speed of 7000 r/min. Figure 2 displays the structure of a typical RIT used in an ORC. Lang et al. developed a 10 kW RIT for waste heat recovery from truck exhaust gases [30]. The RIT was directly connected to a generator. An extra power of 9.6 kW was measured with an isentropic efficiency of 75% when D_4 was used as the working fluid. The turbine can be integrated with the generator and even sometimes with the compressor via a common shaft. The blade height at the inlet of the rotor is small for small-scale RITs, normally in the range of 0.7–1.4 mm. This is not beneficial for efficiency or manufacturing.

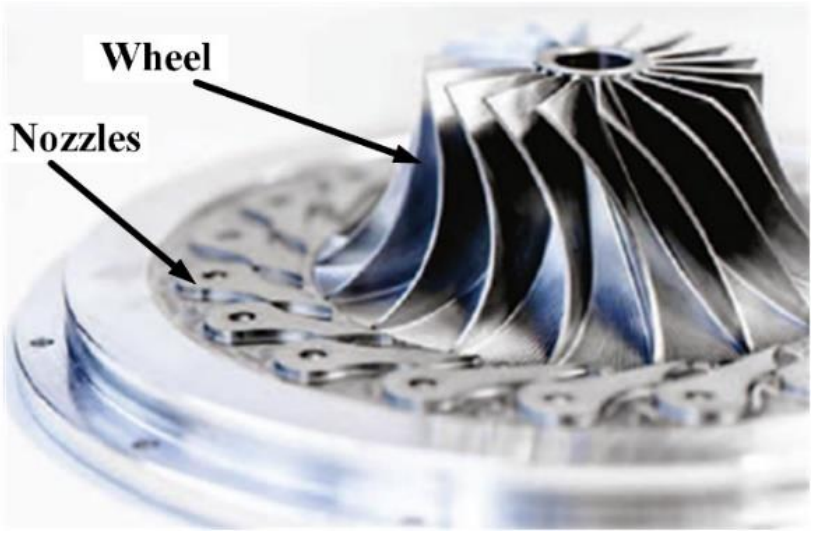

Figure 2. Structure of a typical RIT for a small-scale ORC [37].

The working conditions of ORC must be defined at the design point because the designed critical parameters of RIT are dependent on these inputs. Generally, the decrease in EPR or the inlet temperature is beneficial for the enhancement of turbine efficiency [21], although it is unfavorable for ORC performance. White et al. [38] designed a 25 kW RIT.

As the heat source temperature increased from 80 to 360 °C, the optimized load coefficient increased while the flow coefficient decreased. When the heat source temperature was low, the profile loss was the main part. However, the clearance loss became the largest part when the heat source temperature was high. Sometimes, the operation conditions of ORC may depart from the design point. Therein, the off-design performance of RIT can be evaluated using the mean-line model as well. Persky et al. [39] tried to improve the off-design performance via adjusting the working conditions of ORC. The selection of organic working fluid has a great influence on the results of the preliminary design. The turbine parameters may differ significantly for different organic fluids. Fiaschi et al. [40] designed a 50 kW RIT with regard to six fluids: R134a, R245fa, R1234yf, R236fa, cyclohexane, and n-pentane. The rotor diameters varied from 48 to 138 mm. The RIT using R134a had the smallest diameter, while cyclohexane had the largest. The minimum speed was 31,843 r/min for R1234yf, while it was 54,347 r/min for R134a. Meanwhile, the highest turbine efficiency was 0.83 for R134a, whereas the lowest was only 0.54 for R1234yf. For wet working fluid, cavitation must be avoided during the expansion process to ensure the turbine has enough lifetime [36]. For ORCs with fluctuating heat source temperature or mass flow rate, a variable geometry turbine (VGT) can be employed to improve the power output under the off-design conditions via adjusting the nozzle position [41].

The operation characteristics and optimized performances of RITs can be estimated using the mean-line method. An investigation by Uusitalo et al. [31] indicated that RIT had a higher efficiency when the specific speed was between 0.4 and 0.8. Meanwhile, as the specific speed increased, the losses of clearance and windage decreased, and the largest part was the exit loss. Later, an experimental investigation showed that the turbine could operate at a speed of 12,000–31,000 r/min and the power output reached 6 kW [37]. The mean-line model predicted the performance with high precision. Da Lio et al. [26] studied the preliminary design of RIT based on the Aungier model. The optimal specific speed was found in a narrow range of 0.41–0.42, regardless of the EPR, and the optimal velocity ratio was around 0.70. Hagen et al. [34] designed a RIT with a power output of 140 kW using propane as the working fluid. The inlet and exit pressures of the turbine were 46.6 and 9.58 bars, respectively. The optimized results were consistent with the previous conclusion. RIT is an appropriate choice that can provide high efficiency for most small-scale ORCs. However, for RIT with a high EPR, the performance may decline apparently because the turbine efficiency diminishes owing to supersonic flow losses. For example, if the size of the RIT decreases with a smaller power output, the turbine efficiency will drop, and the speed will obviously increase. Using toluene as the working fluid, Costall et al. [23] designed three RITs. The small turbine had a power output of 15.5 kW at a speed of 136,373 r/min. The blade height at the inlet was only 1.6 mm. The power outputs of the medium and large turbines were 34.1 kW and 45.6 kW, while the turbine speeds were 91,705 r/min and 71,502 r/min, respectively. As the turbine speed decreased, the corresponding turbine efficiency increased from 51.5 to 56.1%. In practice, the Ns-Ds map can be used to select the design point for RIT. Then, the mean-line model can be employed to determine the main geometric parameters. Mounier et al. [42] compared the outcomes from such a map with experimental results, and the deviations were less than 4%.

The effects of designed parameters on the performances of RITs can be estimated based on the mean-line model. An investigation by Rahbar et al. [24] exhibited that the turbine size and power were affected by the load and flow coefficients, turbine speed, EPR, the ratio of vane inlet to exit, the radius of the blade hub at the exit, and the absolute flow angle of the blade. Li et al. [20] analyzed the effects of the reaction degree and the velocity ratio, defined as the peripheral velocity of the rotor to the ideal absolute expansion velocity. The aerodynamic performance was improved as the reaction degree declined. The suitable reaction degree was in the range of 0.3–0.4. Meanwhile, the absolute flow angle of the blade, the relative flow angle, and the wheel diameter ratio also affected the turbine efficiency.

Supersonic flow occurs at a relatively low sonic velocity for organic working fluids. The associated shock and supersonic expansion losses must be taken into account using

the mean-line method. Meroni et al. [29] investigated the preliminary design of RIT with a high EPR. The supersonic losses were modelled. The deviations in turbine efficiency were less than 3% and 5% for design and off-design conditions, respectively. For an ORC with a high EPR, a backswept blade is often employed to decrease the effects of the exiting swirl. Fiaschi et al. [27] compared the design and off-design performances of a 50 kW RIT with and without backswept blades. Supersonic flow occurred inside the RIT with the organic working fluid, and the secondary flow loss was the largest part. The efficiency was improved by 1.5–2.5% for the RIT with backswept blades. More blades were required with a higher load coefficient. Meanwhile, a greater flow deflection angle was obtained, and the absolute flow angle at the exit was also larger. With regard to the supersonic flow at the nozzle exit, Alshammari et al. [22] developed a mean-line model for RIT with backswept blades. The optimized total-to-static efficiency was 74.4% with a power output of 13.6 kW. It is important to select a set of proper decision variables. If inadequate decision variables are chosen, the turbine efficiency might be decreased by almost 8.00% [33].

2.2. Axial Turbine

AT is generally employed for ORCs with a large mass flow rate and a power output ranging from hundreds of kW to several MW. On the other hand, an impulse turbine is suitable for ORCs with a small mass flow. The impulse turbine can connect with a high-speed generator directly with a high EPR, and no axial force occurs. Meanwhile, partial admission can be employed when the mass flow rate is very low [19]. Table 2 lists the performances of ATs in the literature. For large ATs, the power spanned the range of 440 kW–2.446 MW with an efficiency of 0.81–0.891. The corresponding EPR varied from 1.7 to 6.4. The designed turbine speed was located in a relatively narrow interval of 3000–9998 r/min. The turbine speed exhibited a decreasing tendency as the power output increased. For small ATs, the power ranged from 3 kW to 26.3 kW with an efficiency of 0.63–0.80. The EPRs were relatively large (5.62–77.2), and the turbine speed increased significantly to 18,000–91,800 r/min. ATs are normally used in large-scale ORCs. Few investigations concentrated on small-scale ORCs. For industrial waste heat recovery from a micro gas turbine or internal combustion engine, using a working fluid with a low EPR, such as isopentane or isobutane, is beneficial for the design of small ATs [43].

Table 2. Performances of ATs investigated in the literature.

Working Fluid	EPR	Speed (r/min)	Power (kW)	Efficiency (%)	Refs.
R245fa	6.4	9998	1464.6	85.5	[44]
MM	77.2	70,000	26.3	80	[43]
R245fa	6.4	4480	1520	89.1	[45]
R245fa	1.7	9990	440	85.5	[45]
MM	50	91,800	11.2	76.7	[32]
Isobutane	5.8	3000	2446	81	[46]
R113	5.62	18,000	3	63	[47]

The preliminary design of AT based on the mean-line model is mature after many years of development for gas turbines and steam turbines. La Seta et al. [47] developed the program TURAX for the preliminary design of AT. The deviations in total-to-static efficiency were less than 1.3% compared with experimental results. Furthermore, the effects of the designed parameters incorporating stage inlet flow angle, axial velocity, load coefficient, flow coefficient, minimum openings of the nozzle and rotor, nozzle axial chord, opening-to-pitch ratios, and rotational speed were analyzed. Witanowski et al. [48] tried to improve the turbine efficiency via an optimization of over 50 parameters, such as the profiles of the vane and blade, the twisted angle of the blade, the tilt angle, and the axial sweep angle. The optimized efficiency increased from 77.8 to 80.6%. Straight blades are

normally used in ATs. In fact, leaned or twisted blades may be adopted to improve the aerodynamic performance and reduce the flow losses.

Compared with exhaust gases or steam, special attention should be paid during the preliminary design using organic working fluid. The viscosity of organic working fluid is greater than the high-temperature exhaust gases. Hence, the clearance loss of AT using organic working fluid is lower than that of a conventional gas turbine. An investigation showed that the turbine efficiency of organic working fluid decreased by 1.3% for every 1% increment of the tip clearance, while it was 1.5% for conventional gas turbines. The consistencies of the vanes and blades for the ATs using organic working fluid were 1.9–2 and 1.6–2.1, higher than conventional gas turbines at 1.3–1.4 and 1.4–1.7, respectively [49]. Conventional preliminary design defines the load and flow coefficients according to the Smith and Balje map. An investigation by Da Lio et al. [44] indicated that it might not be proper for ATs using organic working fluids. This was because the ranges of the volumetric expansion ratio (VER) and the flow Mach number were much larger than that for conventional gas turbines. Meanwhile, the size of ORC turbine was smaller than gas turbine. The influences of VER and SP were significant on the turbine efficiency. Therefore, a new efficiency map based on the VER and SP was suggested. Later, the effect of the critical temperature (Tc) of organic working fluid was considered, and a correlation as a function of VER, SP, and Tc was proposed [50].

Impulse AT is often employed in small-scale ORC with a high EPR and a small mass flow rate. Recently, Weib et al. [51,52] developed a 13-kW impulse AT using 3D printing. Figure 3 shows the structure of the AT. The turbine wheel is connected directly with the shaft of the generator. Partial admission is beneficial for the reduction of the specific speed. The high-pressure working fluid only enters part of the flow passages along the circumferential direction of the nozzle. Mikielewicz et al. [53] designed a single-stage AT with a power output of 3.35 kW. The corresponding speed was 80,000 r/min. When partial admission was employed, the power output decreased to 2.65 kW while the turbine speed reduced significantly to 40,000 r/min. For small impulse turbines, the effect of the tip clearance becomes more prominent. Klonowicz et al. [54] analyzed the optimal partial admission degrees under different tip clearances. When the tip clearance was 0.15–0.3 mm, the optimal partial admission degree was 0.28, with an efficiency of 65–69%. When the tip clearance decreased, the optimal efficiency would increase by 2–3%, and the associated partial admission degree shifted to the range of 0.3–0.4. For impulse AT, the organic working fluid expands almost completely in the nozzle. Therefore, the supersonic flow in the nozzle should be considered. The compressibility of organic working fluid has a great impact on the turbine's performance. An investigation by Martins et al. [55] showed that the convergent nozzle was only suitable for subcritical ORC with an evaporation temperature less than 140 °C. The convergent-divergent nozzle exhibited a better performance when the evaporation temperature was higher in a supercritical ORC.

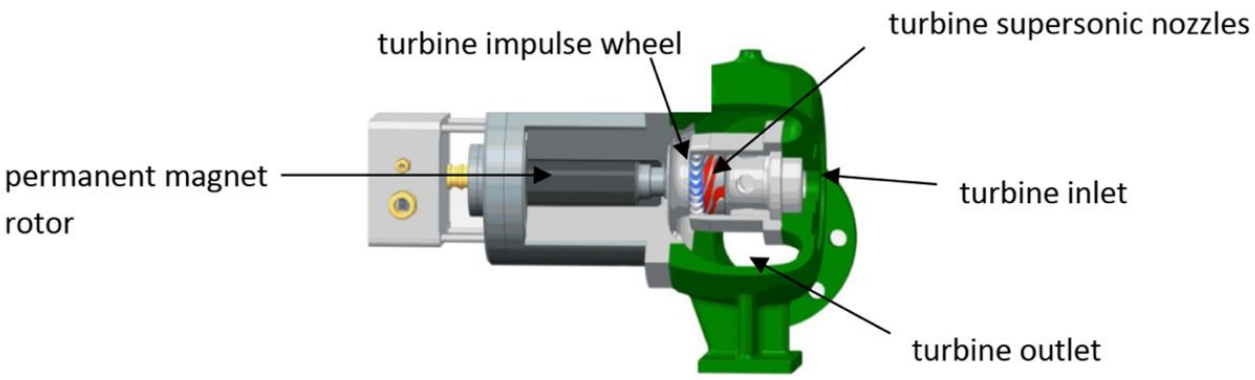

Figure 3. Structure of AT for small-scale ORC [52].

2.3. Radial Outflow Turbine

Exergy S.p.A. [56] developed a prototype of ROT in 2009 for ORC applications. Figure 4 shows the structure of ROT. The vanes of the nozzle and the blades of the rotor are arranged in a ring on the disk, respectively. The organic working fluid flows from the center of the disk through the nozzle and the rotor. Compared with AT, ROT has a more compact size. The high EPR of organic working fluid can be implemented by multistage expansion and a proper configuration of the blade heights. Table 3 lists the investigations of ROTs in the literature. The power outputs of the designed ROTs ranged from 10 kW to 400 kW with an efficiency of 0.687–0.85. The designed speed varied from 7200 r/min to 42,700 r/min. The minimum EPR was 1.47 when R134a was used as the working fluid. For siloxanes, the EPR was as high as 35–45, and a multistage layout was employed.

Table 3. Performances of ROTs investigated in the literature.

Working Fluid	EPR	Speed (r/min)	Power (kW)	Efficiency (%)	Refs.
D_4	45	12,400	10.6	79	[57]
D_4	45	15,400	10.3	77	[57]
MM	35.2	42,700	10	68.7	[32]
R143a	1.47	7200	400	85	[58]

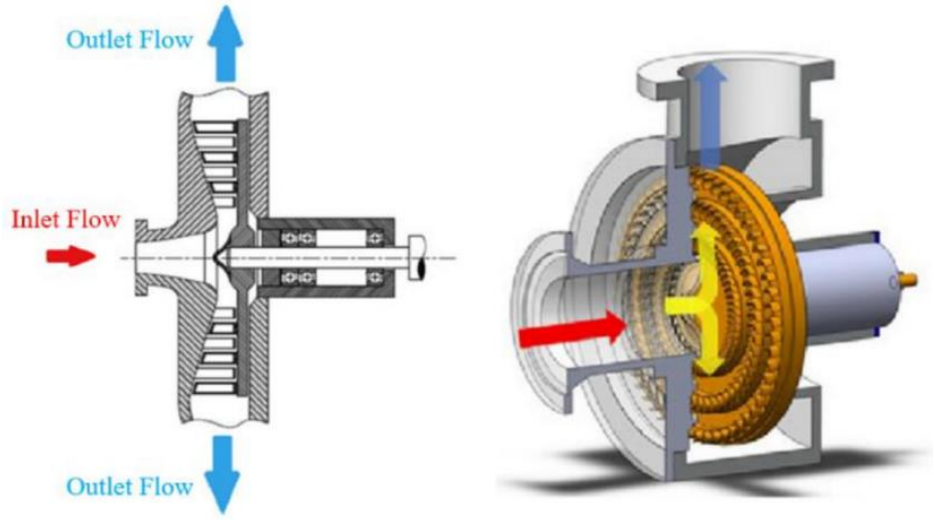

Figure 4. Structure of ROT for ORCs [58].

Conventional mean-line models for ATs are adopted for the preliminary design of the ROT. Currently, no loss model has been developed particularly for ROTs. It should be noted that the repeating stage assumption for ATs cannot be used for ROT due to the radial flow characteristic. Casati et al. [57] designed two 10 kW ROTs based on a mean-line model for small-scale ORC. The five-stage subsonic ROT exhibited an efficiency of 0.79 at a speed of 15,400 r/min. In comparison, the three-stage supersonic ROT had a slightly lower efficiency of 0.77 because of the supersonic flow losses, whereas the speed was much lower at 12,400 r/min. For small ROTs, the specific speed of the first stage deviates apparently against the optimal value due to the geometric constraints, leading to a decrease in the turbine's performance [32]. Meanwhile, the tip clearance loss increases. Kim et al. [58] estimated the off-design performance of a ROT and recommended a suitable range of 0.57–0.70 for the velocity ratio. Accordingly, the optimal load and flow coefficients were 0.85–1.30 and 0.34–0.41, respectively. To reduce the friction loss, a vaneless counter-rotating ROT, known as the Ljungström turbine, can be designed [59]. However, the cost will be increased with a complicated structure, and control is difficult.

2.4. Comparison of Different Turbines

Organic working fluids with a higher molecular weight manifest a smaller enthalpy drop and a greater volumetric ratio during the expansion process compared with exhaust gases. A lower speed of sound is obtained. Meanwhile, fewer stages can be used for turbines using organic fluid. Accordingly, the stage load coefficient is lower with a smaller peripheral velocity. Hence, a low-stress and high-efficiency blade profile can be designed. Nevertheless, the high volume flow ratio is not helpful for the geometric design due to a huge blade height variation and a large flaring angle. Meanwhile, a high supersonic flow loss is not beneficial for the improvement of turbine efficiency. The previous three different turbines have been applied in industry successfully. The companies providing RITs include Atlas Copco, GE Rotoflow, and Cryostar. ATs can be purchased from Ormat and Turboden. Exergy produces ROTs.

Figure 5 shows the distribution of power and rotational speed of different types of turbines investigated in the literature. Most of the turbines are RITs, comprising almost 60%. The power outputs of RITs are relatively small compared with ATs, usually less than 500 kW, and the speed can be as high as 200,000 r/min. In comparison, the power output of ATs can be up to 2.5 MW. However, the speeds of ATs are relatively small, normally less than 50,000 r/min. Both the power and speed of ROTs are relatively small compared with the other two turbines. Figure 6 displays the corresponding data of the efficiency and EPR. The maximum efficiency of RIT is greater than AT, and the peak efficiency of ROT is the lowest. Generally, the efficiency decreases gradually as the EPR increases for all three turbines. AT exhibits the largest EPR. Although the EPR of a RIT can be over 70, most of the EPRs of RITs are less than 10 to maintain an efficiency of greater than 80%. The efficiencies of ROTs are spanned in a narrow range around 80%, although the EPR can vary from 1.47 to 50. The advantages and disadvantages of RIT, AT, and ROT are compared in Table 4. Each type of turbine has its own advantages. In practice, the most suitable turbine should be selected according to the specific requirements of ORC system. Not only the aerodynamic performance but also other indexes such as cost and availability from the market must be estimated.

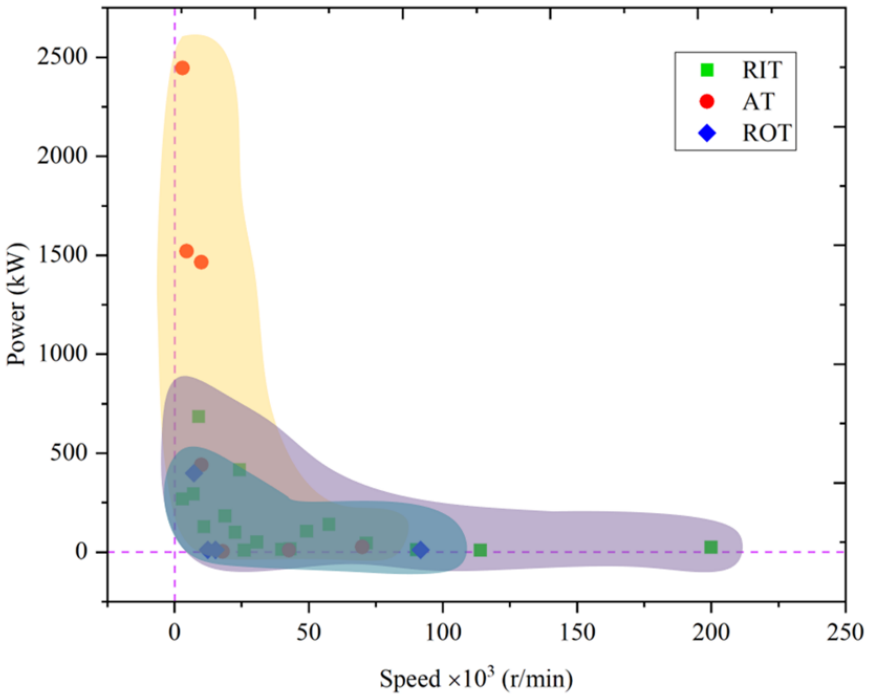

Figure 5. Distribution of power output and speed for different turbines designed in the literature.

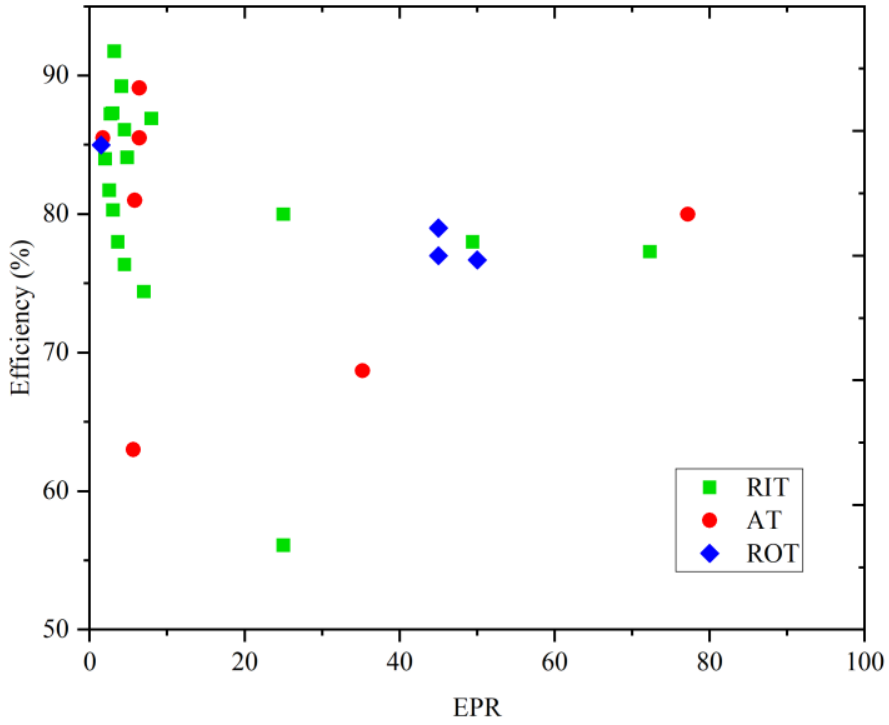

Figure 6. Distribution of corresponding efficiency and EPR for different turbines.

Table 4. Comparison of advantages and disadvantages of different turbines.

Turbine	Advantages	Disadvantages
RIT	• High efficiency due to the decrease in radius from the inlet to the exit of the rotor; • Large single-stage EPR, which normally can be up to 10; • VGT technology can be employed to improve off-design performance; • Suitable for turbines with a power output of several to hundreds of kW.	• Low reaction degree of the rotor; • High Mach number may occur at the stator exit, and a large supersonic flow loss; • High speed and sometimes a reducer are required to connect with the generator; • Limited volumetric expansion ratio and mass flow rate.
AT	■ Mature technology, multi-stage AT, covers 90% of the market for power generation; ■ High specific speed; ■ Stage load coefficient can be decreased via a multi-stage arrangement; ■ Suitable for ORCs with hundreds of kW to several MW power output.	■ Small volumetric expansion ratio constrained by h/D; ■ Low blade height in the first stage may cause a high secondary loss; ■ Large blade height of the last stage may need twisted blades; ■ Supersonic flow may occur at the stator exit, causing shock loss; ■ Small ATs have a low efficiency because of their increased profile and leakage losses.
ROT	◆ Mean diameter increases during the expansion process, hence the blade height increases for the first stage and decreases for the last stage, a better accommodation of a large volumetric expansion ratio with a limited flaring angle; ◆ Moderate aspect ratio, multiple stages can be arranged on one disk to avoid supersonic flow; ◆ High stage reaction degree, low load, and flow coefficients; ◆ Low speed, small vibration, good rotor dynamics.	◆ Specific work is lower than RIT and AT; ◆ Bending moment caused by the centrifugal force of the overhung blade; ◆ Rotor inlet radius is smaller than the exit, leading to a high meridional velocity at the inlet of the rotor.

3. Loss Model

3.1. Models for RIT

The velocity triangles are determined based on a set of parameters, such as load and flow coefficients and reaction degrees, during the preliminary design. Accordingly, the main geometry parameters, such as the blade height, axial chord, blade pitch, and absolute flow angles of the nozzle and rotor, are obtained. On the other hand, to predict the turbine efficiency, models for the losses that occurred during the expansion process are required for the mean-line method. The loss models for ATs are relatively mature. However, various loss models have been employed for RITs using organic working fluids. It is necessary to give a summary of these models.

The simplest method estimates the flow loss of RIT based on a friction model [20]. For instance, Han et al. [21] calculated the loss coefficients of the nozzle and the rotor based on the velocity coefficient, and then the peripheral efficiency was determined. Such a simple model has a relatively large deviation for turbine performance prediction. Most investigations divided the flow losses according to the physical characteristics of the flow process, such as incidence loss, passage loss, tip clearance loss, windage loss, and exit loss. The Baines model is often employed to model these losses [36], which mainly consist of incidence loss, passage loss, tip clearance loss, and windage loss. Table 5 lists the model developed by Meroni et al. [29], which is mainly based on the equations of the Baines model. ZTurbo is software developed specially for ORC turbine design [32]. In this software, the Baines model can be chosen to estimate the turbine efficiency and optimize the turbine geometry in the preliminary design process. Suhrmann's model [60] accounted for the skin friction loss, secondary flow loss, incidence loss, tip clearance loss, and exit loss, which were also employed in the mean-line model of RIT for ORCs [39,61]. Table 6 lists a model developed based on the Suhrmann model. Rodgers model [62] estimated the flow loss according to the turbine geometry and the operation conditions, which had better precision when the chord ratio was less than 2% and the Mach number was lower than 1.2 [33]. Table 7 gives the loss model developed by Fiaschi et al. [27], which is mainly based on the Rodgers model. For the passage loss of the rotor, correlations were used to represent the losses caused by the high curvature of the profile and the pressure gradient, as well as the skin friction, respectively. Meanwhile, the flow loss in the diffuser was also modelled in terms of the friction loss and the enlargement of the section loss. The Rohlik model [63] was also used to model the flow losses of RIT.

Table 5. Loss model for preliminary design of RIT adopted by Meroni et al. [29].

Description	Equation	Refs.
Nozzle passage	$\Delta h_{p,n} = k_{p1}\frac{0.05}{Re_3^{0.2}}\left[\frac{3\tan\alpha_3}{s_3/c_n}+\frac{s_3 cos\alpha_3}{b_3}\right]\frac{1}{2}C_3^2$	Rodgers [62]
Nozzle trailing edge	$\Delta h_{t,n} = \left(\frac{Z_N t_3}{2\pi r_3 cos\alpha_3}\right)^2\frac{1}{2}C_3^2 Y_3$	Glassman [64]
Nozzle post-expansion	$\Delta h_{pe,n} = \left(\frac{M_3-M_2}{M_3}\right)^2\frac{1}{2Y_3}C_3^2$	Aungier [65]
Interspace	$\Delta h_{VS} = k_{VS}C_f\left(\frac{L}{D}\right)\frac{1}{2}\left(\frac{C_3+C_4}{2}\right)^2$	Kastner and Bhinder [66]
Incidence	$\Delta h_i = k_i\left(sin\left\|\beta_4-\beta_{4,opt}\right\|\right)^2\frac{1}{2}W_4^2$	Baines [67]
Passage	$\Delta h_{p,r} = k_p\left\{k_{p2}\left(\frac{L_H}{D_H}\right)+0.68k_{p3}\left[1-\left(\frac{r_{6rms}}{r_4}\right)^2\right]\left(\frac{cos\beta_6}{b_6/c_r}\right)\right\}\frac{1}{2}\left(W_4^2+W_6^2\right)$	Baines [67]
Clearance	$\Delta h_c = \left(U_4^3 Z_R/8\pi\right)\left(0.4\varepsilon_x C_x+0.75\varepsilon_r C_r-0.3\sqrt{\varepsilon_x\varepsilon_r C_x C_r}\right)$	Baines [67]
Trailing edge	$\Delta h_{t,r} = \left(\frac{Z_R t_6}{\pi(r_{6s}+r_{6h})cos\beta_6}\right)^2\frac{1}{2}W_6^2 Y_6$	Glassman [64]
Post-expansion	$\Delta h_{pe,r} = \left(\frac{M_{6,rel}-M_5}{M_{6,rel}}\right)^2\frac{1}{2Y_6}W_6^2$	Aungier [65]
Windage	$\Delta h_w = \frac{0.25k_f\bar{\rho}U_4^3 r_4^2}{\dot{m}}$	Daily and Nece [68]

Table 6. Loss model for preliminary design of RIT adopted by Rahbar et al. [24].

Description	Equation	Refs.
Volute	$\Delta h_V = k_v C_2^2/2$	Baines [67]
Nozzle	$\Delta h_N = 4 f_N \bar{C}^{-2} \frac{L_N}{D_N}$	Whitfield [69]
Incidence	$\Delta h_i = W_{\theta 4}^2/2$	Whitfield [70]
Secondary	$\Delta h_s = \frac{C_4^2 d_4}{Z_R r_c}$	Rodgers [71]
Friction	$\Delta h_f = f\left(1+0.075\bar{Re}^{-0.25}\sqrt{\frac{D_R}{2r_c}}\right)\left[\bar{Re}\left(\frac{d_4}{2r_c}\right)\right]^{0.05}\left[\frac{W_4+\frac{1}{2}(W_{5t}+W_{5h})}{2}\right]^2 \frac{L_R}{D_R}$	Suhrmann [60]
Leakage	$\Delta h_c = \left(U_4^3 Z_R/8\pi\right)\left(0.4\varepsilon_x C_x + 0.75\varepsilon_r C_r - 0.3\sqrt{\varepsilon_x \varepsilon_r C_x C_r}\right)$	Baines [67]
Exit	$\Delta h_{exit} = 0.5 C_5^2$	
Windage	$\Delta h_w = \frac{k_f \bar{\rho} U_4^3 r_4^2}{4\dot{m}}$	Daily and Nece [68]

Table 7. Loss model for preliminary design of RIT developed by Fiaschi et al. [27].

Description	Equation	Refs.
Diffuser	$\xi_D = k\xi_{en} + \xi_f$ $\xi_{en} = 3.2 tg\frac{\gamma_D}{2}\sqrt[4]{tg\frac{\gamma_D}{2}}\left(1-\frac{A_3}{A_4}\right)^2$ $\xi_f = \frac{f_D}{8 sin\frac{\gamma_D}{2}}\left[1-\left(\frac{A_3}{A_4}\right)^2\right]$	Runstadler [72]
Nozzle	$\xi_N = \frac{0.05}{Re^{0.2}}\left[\frac{3tg\alpha_2}{s/x} + \frac{scos\alpha_2}{b_3}\right]$	Rodgers [62]
Incidence	$\Delta h_i = \frac{1}{2}\left(W_2 sin\beta_2 - W_2 sin\beta_{2,opt}\right)^2$	NASA [73]
Friction	$\xi_{R,f} = \frac{\lambda_R L_R^*}{D_R^*}$	Benson [74]
Leakage	$\Delta q_c = 0.4\frac{\varepsilon}{b_2}\left(\frac{C_{u2}}{U_{t,le}}\right)^2$	Rodgers [62]
Profile	$\Delta q_p = 0.5\left(\frac{\frac{b_2}{r_2}+\frac{b_3}{r_2}}{1-\left(\frac{r_3}{r_2}\right)^2}\right)\left(\frac{W_2^2+W_3^2}{2a_{01}^2}\right)\left(\frac{a_{01}^2}{U_2^2}\right)$ $\Delta q_{bl} = \frac{2(C_{\theta 2}/U_2)^2}{Z_R Z/r_2}$	Whitfield [75]
Windage	$\Delta q_w = \frac{0.25\bar{\rho} U_2 r_2^2 k_f}{\dot{m}}$	Daily and Nece [68]

Currently, a uniform and standard model acknowledged by all researchers does not exist for RITs. The results of different correlations may differ significantly from each other, although the final predictions of turbine efficiency are approximate. Many investigations only considered part of the components of the turbine, which normally consist of the volute, nozzle, rotor, and diffuser. Tables 5–7 give three typical models. Table 8 shows another model developed by Erbas and Biyikoglu [36] in which all four main components were modelled. Compared with the rotor, the losses of the other components might be much less. Hence, many investigations neglected these losses. However, for RITs with a high EPR, the flow losses from the other parts, such as nozzle, cannot be ignored [29]. Similar models as the rotor can be used to estimate the flow losses in the nozzle, such as passage loss, trailing edge loss, and post-expansion loss.

The incidence loss is normally determined according to the Baines model. In [23], the following equation from [73] was employed:

$$\Delta h_i = \frac{1}{2} W_2^2 (1 - cos^n i_2) \quad (1)$$

where n is 2.5 if $i > 0$, otherwise n = 1.75.

Table 8. Loss model for preliminary design of RIT adopted by Erbas and Biyikoglu [36].

Description	Equation	Refs.
Volute	$L_V = 0.054(\rho_{in} C_0 2 r_{in}/\mu)^{-0.25} \pi C_0^2/2$	Baines [67]
Nozzle	$L_N = C_{in}^2(1-\phi_N^2)/(2\phi_N^2)$	Baines [67]
Incidence	$L_i = (1/2) W_{in}^2 sin^2\left(\beta_{in} - \beta_{in,opt}\right)$	Wasserbauer and Glassman [76]
Profile	$L_p = 0.15\left[W_{in}^2 cos^2\left(\beta_{in} - \beta_{in,opt}\right) + W_{exit}^2\right]$	Wasserbauer and Glassman [76]
Leakage	$L_c = \left(U_4^3 Z_R/8\pi\right)\left(0.4\varepsilon_x C_x + 0.75\varepsilon_r C_r - 0.3\sqrt{\varepsilon_x \varepsilon_r C_x C_r}\right)$	Baines [67]
Diffuser	$L_D = C_{exit}^2(1-C_D)/2$	

With regard to the tip clearance loss, some researchers employed the correlation of Krylov and Spunde [77] that only accounted for the effects of radial clearance. However, the Dambach correlation [78] was adopted by most investigations in which both the radial and axial clearances were considered. For the windage loss, the following equation [79] was also used.

$$\Delta h_{win} = \frac{0.56\rho_2 D_2^2 (U_2/100)^3}{\dot{m} Re} \tag{2}$$

The trailing edge loss accounts for the flow loss downstream of the throat. In [28], the Ghosh correlation [80] was employed with respect to the effects of the relative Mach number at the exit.

$$\Delta h_t = \frac{2}{\gamma M_{6,rel}^2} \frac{P_{06,rel}}{P_6\left[1 + W_{6,rms}^2/(2T_6 c_p)\right]^{\left(\frac{\gamma}{\gamma-1}\right)}} \tag{3}$$

The models for the incidence loss, passage loss, trailing edge loss, tip clearance loss, windage loss, and exit loss were reviewed by Persky et al. [81]. However, for turbines used in small-scale ORCs, a high EPR is required, and supersonic flow often occurs. It is necessary to give a new summary, especially for the losses associated with the supersonic flow, including the shock loss at the inlet and the supersonic expansion loss in the proximity of the exit. If the losses are modelled properly, the mean-line model can predict the turbine efficiency with high precision. Deviations can be less than 2% compared with the results of CFD. However, it is impossible to predict all these flow losses accurately using the mean-line model, and many empirical constants need to be validated further for turbines using organic working fluids. Meroni et al. [22] developed a mean-line model for RIT with a high EPR. The Glassman correlation was employed to determine the trailing edge loss. The post-expansion loss was modelled by the Aungier model. The detailed equations are listed in Table 9. This mean-line model was also adopted by Hagen et al. [34] and Wang et al. [35].

Conventional turbines are developed only for subsonic conditions. As technology develops, the supersonic flow losses should be considered as well. Supersonic flow is more prone to appear in the turbines used for ORCs. For RITs, the Aungier model is widely employed to estimate the supersonic losses [26,82]. Table 9 lists the main equations for the flow losses developed by Da Lio et al. [19] based on the Aungier model. The loss coefficients of total pressure are used to model each item. The profile loss is expressed based on the boundary layer theory. The circumferential distortion loss is calculated with regard to the mixing losses with non-uniform angular motion. The losses of the rotor incorporate the incidence loss, blade loading loss, and hub-to-shroud loading loss. When supersonic flow occurs in the turbine, the shock loss at the leading edge and the post-expansion loss due to the supersonic flow are modelled respectively.

Table 9. Loss model for preliminary design of RIT developed by Da Lio et al. [26] based on the Aungier model.

Description	Equation
Volute	$Y_v = \frac{2\Theta_v + \Delta_v^2}{(1-\Delta_v)^2} + \left(\frac{\frac{r_{1v}C_{1v}}{r_{3v}} - C_{t3v}}{C_{3v}} \right)^2$
Nozzle	Subsonic flow: $Y_n = \frac{2\Theta_n + \Delta_n^2}{(1-\Delta_n)^2} + sin^2\left(\alpha_{1n} - \alpha_{1n}^*\right) \frac{p_{01n} - p_{1n}}{p_{03n} - p_{3n}}$
	Supersonic flow: $Y_{n\|M_{3n}>1} = Y_{n\|M_{3n}=1} + \left(\frac{M_{3n}-1}{M_{3n}} \right)^2$
Interspace	$Y_a = \frac{2\Theta_a + \Delta_a^2}{(1-\Delta_a)^2} + \left[\left(\frac{A_{1a}}{A_{3a}} - 1 \right) sin\alpha_{1a} \right]^2 \frac{p_{01a} - p_{1a}}{p_{03a} - p_{3a}}$
Incidence	$Y_i = sin^2\left(\alpha_{1r} - \alpha_{1r}^*\right) \frac{p_{01r} - p_{1r}}{p_{03r} - p_{3r}}$
Profile	$Y_p = \frac{2\Theta_r + \Delta_r^2}{(1-\Delta_r)^2}$
Blade loading	$Y_{bl} = \frac{1}{24} \left(\frac{\Delta W}{W_{3r}} \right)^2$
Hub-to-shroud loading	$Y_{hs} = \frac{1}{6} \left(\frac{\kappa_m b_{3r} W_{2r}}{W_{3r} sin\alpha_{3r}} \right)^2$
Leakage	$Y_c = \frac{\dot{m}_{CL} \Delta p}{\dot{m}(p_{03r} - p_{3r})}$
Windage	$\Delta h_w = \frac{1}{6} \frac{C_M \bar{\rho} \omega^3 r_{1r}^5}{\dot{m}}$

3.2. Models for AT and ROT

The mean-line models for conventional ATs are well developed, using exhaust gases or high-temperature steam as working fluid. The loss models for ATs using organic working fluid are basically the same as the conventional models, which can be mainly categorized into three types: the Ainley and Mathieson (AM) model [83] and subsequently corrected models, such as the Dunham and Came (DC) model [84] and the Kacker and Okapuu (KO) model [85], the Craig and Cox (CC) model [86], and the Aungier model [65]. The DC model corrected the profile loss according to the Mach number at the exit based on the AM model. Meanwhile, the effects of aspect ratio on the secondary loss and the power law dependence of the tip clearance loss were considered. The AM and DC models were developed for turbines with subsonic flow. The KO model further added the shock loss and the compressibility effect correction for profile loss. The secondary loss was corrected with regard to the blades with a low aspect ratio and the compressibility effect as well. The CC model split the losses into profile, secondary, and annulus, due to sudden enlargement in the flow path or wall cavity. Meanwhile, other losses, such as leakage, disk windage, wetness, and partial admission, were also incorporated. Similar to the DC model, the CC model did not consider the supersonic flow. Other equations must be integrated if supersonic flow loss cannot be ignored [47,87].

In the Aungier model, the losses for the profile, secondary flow, trailing edge, post-expansion, shock wave, and tip clearance were modelled. Da Lio et al. [44] and Peng et al. [88–90] used the Aungier model to design different ATs. In [45], Salah et al. compared the results of the DC, KO, CC, and Aungier models. It seemed that the differences among these models were small for the prediction of the turbine efficiency. A maximum percentage of 1.5% and 3.7% in the total-to-total and total-to-static efficiencies were obtained, respectively. For small-scale ATs in ORCs, the KO and Aungier models are recommended, which account for the flow losses under supersonic conditions. Wei [91] summarized various loss models for ATs, including Soderberg, Traupel, AM, DC, KO, CC, Denton, Stewart, Balje and Binsley, Zehner, Moustapha, Ito, and Lakshminarayana, and could be referenced.

Currently, the loss models for ROTs are drawn from those of ATs. In [58], the simple Soderberg model was employed to determine the efficiency. In the software ZTurbo, the Traupel model was integrated for the preliminary design of ROT with organic working fluid. The results of Casati et al. [57] showed that the efficiency curves of the CC and Traupel models were approximate for a three-stage ROT. Although the flow in ROT is similar

with AT. Some discrepancies exist, and further investigations are required to validate the accuracy of the loss models.

4. Optimization Algorithm

The preliminary design searches in a space defined by a set of decision variables such as the stage load and flow coefficients, reaction degree, blade height, axial length, and inlet blade angle to minimize the total loss. Therefore, a multivariable optimization algorithm needs to be integrated to obtain the global optimal solution. Generally, there are two approaches: the gradient-based search algorithm and the stochastic optimization method. In the optimization toolbox of Matlab, some functions can be employed to optimize the nonlinear mean-line model. Fmincon is such a simple function and has been used in [89] for the preliminary design of multi-stage ATs and small-scale impulse turbines. Alshammari et al. [22] used Fmincon to maximize the target as a combination of the total-to-static efficiency, power output, and turbine size. The GlobalSearch function was also adopted [38,42], which is a nonlinear programming optimization method with multiple start points that can be used to obtain the global optimum. The sequential quadratic programming is conducted at each step in this algorithm. Other nonlinear gradient-based optimization algorithms might be employed as well. For instance, the NLPQL function [92] was employed by Hagen et al. [34] and a second-order central difference approximation was designed together with equality constraints to decrease the computation load.

The genetic algorithm (GA) as a random optimization method has been widely employed in mean-line models [25,39,93]. Turbine efficiency is often set as the target of a simple single-objective optimization. In [57], ZTurbo was coupled to the external optimizer Dakota that GA was employed. The total-to-static efficiency was maximized, and the decision variables incorporated the load and flow coefficients, with the shape factor accounting for the blade height and chord length. In [29], GA was adopted to optimize the RIT with a high EPR. Zhai et al. [94] optimized six design parameters of RIT for a low-temperature ORC, and the efficiency increased from 88.06% to 91.01% after the optimization. Multiple population GA can be adopted to avoid convergence to the local extreme point [95]. Multi-objective optimization is normally implemented with the Non-dominated Sorting Genetic Algorithm-II (NSGA-II) method. Turbine efficiency, cost or size are configured as two optimization objectives [33]. In practice, off-design performance may also need to be considered for some ORCs that operate frequently under such conditions. In [36], both the efficiencies at the design point and one selected off-design point were specified as the objectives. The turbine geometry was optimized according to the resulted Pareto front. To improve the performance of ORC, a combined optimization of ORC and the turbine is necessary. In [96], NSGA-II was employed to optimize the ORC system model in combination with a mean-line model of RIT.

Similar to GA, particle swarm optimization (PSO) is another stochastic algorithm that can be used in the preliminary design regardless of the continuity and derivability of the nonlinear function. Compared with GA, the optimization principle of PSO is simpler, the equations are simpler, and the convergence speed is quicker. Han et al. [21] optimized the geometry of RIT based on eight decision variables, including degree of reaction, velocity ratio, stator velocity coefficient, rotor velocity coefficient, wheel diameter ratio, absolute velocity angle at the rotor inlet, relatively velocity angle at the rotor outlet, and rotational speed. However, for high-dimensional, complicated problems, GA and PSO might encounter premature or poor convergence, and the global optimum cannot be guaranteed. The DIRECT algorithm [97], a modified version of Lipschitzian optimization, can be employed to avoid these issues effectively [24]. This algorithm can search multiple local optima via continuously dividing hyperrectangles in a hyperspace. The accuracy of DIRECT is better than GA, although the convergence speed is slower.

5. Summary, Challenges, and Research Directions

The mean-line method was reviewed for the design of various turbines for ORC systems. The performances of the designed RITs, ATs, and ROTs were analyzed. The main conclusions, challenges, and future research directions are summarized as follows:

(1) For medium and small ORC systems with a power output of up to hundreds of kW, RIT is preferred if the EPR is less than 10. RIT takes advantage of high efficiency and high-stage EPR compared with AT and ROT. However, the exit flow velocity is large with a high rotational speed. Conventional techniques that have been used to improve the performance of RIT. As the EPR increases, backswept blades and split blades can be employed. Meanwhile, a supersonic nozzle design is required if the EPR is very high. VGT can be employed to improve the off-design performance of RIT. In addition, suitable manufacturing technology for supersonic RIT used in ORC with a high EPR needs to be developed. 3D printing may be a good solution, while further experimental testing is required.

(2) For large-scale ORCs, multi-stage AT is recommended that has a high efficiency under the conditions with a large mass flow rate. However, the EPR of each stage is small. When the mass flow rate is low, the secondary loss and the clearance loss are high due to the low blade height. For small-scale ORCs with a very high EPR and a very small mass flow rate, AT with an impulse stage is promising. Partial admission can be employed to avoid a very small blade height, decrease the rotational speed, and adapt to a wide variation of the operation conditions. Large-scale ATs are mature technologies. However, for small-scale ATs, further investigations are required to improve the efficiency, especially for the impulse AT with one or two stages.

(3) Siloxanes normally have a very high EPR, and ROT is suitable. All the stages can be arranged on one disk, and the blade height of the first row can be maintained at a relatively high level. However, the exit flow velocity is evidently greater than the inlet velocity, leading to a low efficiency. Meanwhile, high stress occurs at the blade hub. The aerodynamic performances of ROTs for various organic working fluids need to be estimated comprehensively. In addition, the performance of the vaneless, counter-rotating Ljungström turbine should be explored for ORC applications.

(4) With regard to the preliminary design of ORC turbines, the mean-line models for ATs are mature, and Aungier and KO models are recommended that can predict the supersonic flow loss with high accuracy. Regarding the loss models of RIT, the models of Baines, Suhrmann, and Rodgers are optional. Empirical correlations are normally employed in mean-line models. These correlations are developed mainly using exhaust gases or steam as the working fluid. The feasibility and precision when organic working fluids are employed need to be further validated via experimental data or CFD simulations. Because ORC turbines have a low sonic speed and are prone to the occurrence of shock waves, further investigations are needed to develop associated loss models with high precision regarding the real gas effects of organic working fluids.

(5) The preliminary design of the ORC turbine is a multivariable optimization problem based on the mean-line method. A gradient-based algorithm may encounter convergence issues. Local optima may be obtained by a GA or PSO algorithm. For such a highly nonlinear multivariable optimization problem, stochastic optimization such as GA and PSO is recommended, and multiple initial points are suggested to validate the global optimal results. Not only the turbine efficiency but also other factors such as the size and cost must be estimated. Another important direction is the combined optimization of ORC and turbine. The decision variables will obviously increase, and the computation complication will soar. However, it is useful for the implementation of the actual ORC system.

(6) Finally, small-scale turbines face great difficulties in manufacturing and cost reduction. A generator is often connected directly with an ORC turbine, and a compact integrated component can be installed. A high-speed generator with a speed over 30,000 r/min

is difficult to manufacture. Organic working fluids may be toxic or flammable. A rigid requirement for the sealing of the turbine must be guaranteed. Therefore, many engineering issues need to be solved before the wide application of small-scale ORCs.

Author Contributions: Conceptualization, E.W.; methodology, E.W. and N.P.; formal analysis, E.W. and N.P.; investigation, E.W. and N.P.; resources, N.P.; data curation, E.W.; writing—original draft preparation, N.P.; writing—review and editing, E.W.; supervision, E.W.; funding acquisition, E.W. All authors have read and agreed to the published version of the manuscript.

Funding: This research was funded by the National Natural Science Foundation of China, grant number 51876009.

Data Availability Statement: Not applicable.

Conflicts of Interest: The authors declare no conflict of interest.

References

1. Hu, S.; Yang, Z.; Li, J.; Duan, Y. A review of multi-objective optimization in Organic Rankine Cycle (ORC) system design. *Energies* **2021**, *14*, 6492. [CrossRef]
2. Loni, R.; Mahian, O.; Markides, C.N.; Bellos, E.; Le Roux, W.G.; Kasaeian, A.; Najafi, G.; Rajaee, F. A review of solar-driven organic Rankine cycles: Recent challenges and future outlook. *Renew. Sustain. Energy Rev.* **2021**, *150*, 111410. [CrossRef]
3. Loni, R.; Mahian, O.; Najafi, G.; Sahin, A.Z.; Rajaee, F.; Kasaeian, A.; Mehrpooya, M.; Bellos, E.; le Roux, W.G. A critical review of power generation using geothermal-driven organic Rankine cycle. *Therm. Sci. Eng. Prog.* **2021**, *25*, 101028. [CrossRef]
4. Tian, H.; Liu, P.; Shu, G. Challenges and opportunities of Rankine cycle for waste heat recovery from internal combustion engine. *Prog. Energy Combust. Sci.* **2021**, *84*, 100906. [CrossRef]
5. Wang, E.; Peng, N.; Zhang, M. System design and application of supercritical and transcritical CO_2 power cycles: A review. *Front. Energy Res.* **2021**, *9*, 723875. [CrossRef]
6. Loni, R.; Najafi, G.; Bellos, E.; Rajaee, F.; Said, Z.; Mazlan, M. A review of industrial waste heat recovery system for power generation with Organic Rankine Cycle: Recent challenges and future outlook. *J. Clean. Prod.* **2021**, *287*, 125070. [CrossRef]
7. Mukhtar, M.; Adebayo, V.; Yimen, N.; Bamisile, O.; Osei-Mensah, E.; Adun, H.; Zhang, Q.; Luo, G. Towards Global Cleaner Energy and Hydrogen Production: A Review and Application ORC Integrality with Multigeneration Systems. *Sustainability* **2022**, *14*, 5415. [CrossRef]
8. Imran, M.; Usman, M.; Park, B.-S.; Lee, D.-H. Volumetric expanders for low grade heat and waste heat recovery applications. *Renew. Sustain. Energy Rev.* **2016**, *57*, 1090–1109. [CrossRef]
9. Talluri, L.; Dumont, O.; Manfrida, G.; Lemort, V.; Fiaschi, D. Experimental investigation of an Organic Rankine Cycle Tesla turbine working with R1233zd(E). *Appl. Therm. Eng.* **2020**, *174*, 115293. [CrossRef]
10. Alshammari, F.; Karvountzis-Kontakiotis, A.; Pesyridis, A.; Usman, M. Expander Technologies for Automotive Engine Organic Rankine Cycle Applications. *Energies* **2018**, *11*, 1905. [CrossRef]
11. Quoilin, S.; Declaye, S.; Legros, A.; Guillaume, L.; Lemort, V. Working fluid selection and operating maps for Organic Rankine Cycle expansion machines. In Proceedings of the 21st International Compressor Conference, West Lafayette, IN, USA, 16–19 July 2012.
12. Colonna, P.; Casati, E.; Trapp, C.; Mathijssen, T.; Larjola, J.; Turunen-Saaresti, T.; Uusitalo, A. Organic Rankine Cycle Power Systems: From the Concept to Current Technology, Applications, and an Outlook to the Future. *J. Eng. Gas Turbines Power* **2015**, *137*, 100801. [CrossRef]
13. Bao, J.; Zhao, L. A review of working fluid and expander selections for organic Rankine cycle. *Renew. Sustain. Energy Rev.* **2013**, *24*, 325–342. [CrossRef]
14. Rahbar, K.; Mahmoud, S.; Al-Dadah, R.K.; Moazami, N.; Mirhadizadeh, S.A. Review of organic Rankine cycle for small-scale applications. *Energy Convers. Manag.* **2017**, *134*, 135–155. [CrossRef]
15. Qyyum, M.A.; Khan, A.; Ali, S.; Khurram, M.S.; Mao, N.; Naquash, A.; Noon, A.A.; He, T.; Lee, M. Assessment of working fluids, thermal resources and cooling utilities for Organic Rankine Cycles: State-of-the-art comparison, challenges, commercial status, and future prospects. *Energy Convers. Manag.* **2022**, *252*, 115055. [CrossRef]
16. Pethurajan, V.; Sivan, S.; Joy, G.C. Issues, comparisons, turbine selections and applications—An overview in organic Rankine cycle. *Energy Convers. Manag.* **2018**, *166*, 474–488. [CrossRef]
17. Zhao, Y.; Liu, G.; Li, L.; Yang, Q.; Tang, B.; Liu, Y. Expansion devices for organic Rankine cycle (ORC) using in low temperature heat recovery: A review. *Energy Convers. Manag.* **2019**, *199*, 111944. [CrossRef]
18. Zywica, G.; Kaczmarczyk, T.Z.; Ihnatowicz, E. A review of expanders for power generation in small-scale organic Rankine cycle systems: Performance and operational aspects. *Proc. Inst. Mech. Eng. Part A J. Power Energy* **2016**, *230*, 669–684. [CrossRef]
19. Weib, A.P. Volumetric expander versus turbine-which is the better choice for small ORC plants? In Proceedings of the 3rd International Seminar on ORC Power Systems, Brussels, Belgium, 12–14 October 2015.

20. Li, C.; Guo, Z.; Guo, H.; Bao, X.; Zhou, L. Influences of main design parameters on the aerodynamic performance of a micro-radial inflow turbine. *AIP Adv.* **2022**, *12*, 105012. [CrossRef]
21. Han, Z.H.; Jia, X.Q.; Li, P. Preliminary design of radial inflow turbine and working fluid selection based on particle swarm optimization. *Energy Convers. Manag.* **2019**, *199*, 111933. [CrossRef]
22. Alshammari, F.; Karvountzis-Kontakiotis, A.; Pesyridis, A.; Alatawi, I. Design and study of back-swept high pressure ratio radial turbo-expander in automotive organic Rankine cycles. *Appl. Therm. Eng.* **2019**, *164*, 114549. [CrossRef]
23. Costall, A.W.; Hernandez, A.G.; Newton, P.J.; Martinez-Botas, R.F. Design methodology for radial turbo expanders in mobile organic Rankine cycle applications. *Appl. Energy* **2015**, *157*, 729–743. [CrossRef]
24. Rahbar, K.; Mahmoud, S.; Al-Dadah, R.K.; Moazami, N. Modelling and optimization of organic Rankine cycle based on a small-scale radial inflow turbine. *Energy Convers. Manag.* **2015**, *91*, 186–198. [CrossRef]
25. Rahbar, K.; Mahmoud, S.; Al-Dadah, R.K.; Moazami, N. Parametric analysis and optimization of a small-scale radial turbine for Organic Rankine Cycle. *Energy* **2015**, *83*, 696–711. [CrossRef]
26. Da Lio, L.; Manente, G.; Lazzaretto, A. A mean-line model to predict the design efficiency of radial inflow turbines in organic Rankine cycle (ORC) systems. *Appl. Energy* **2017**, *205*, 187–209. [CrossRef]
27. Fiaschi, D.; Manfrida, G.; Maraschiello, F. Design and performance prediction of radial ORC turboexpanders. *Appl. Energy* **2015**, *138*, 517–532. [CrossRef]
28. Jung, H.-C.; Krumdieck, S. Meanline design of a 250 kW radial inflow turbine stage using R245fa working fluid and waste heat from a refinery process. *Proc. Inst. Mech. Eng. Part A J. Power Energy* **2016**, *230*, 402–414. [CrossRef]
29. Meroni, A.; Robertson, M.; Martinez-Botas, R.; Haglind, F. A methodology for the preliminary design and performance prediction of high-pressure ratio radial-inflow turbines. *Energy* **2018**, *164*, 1062–1078. [CrossRef]
30. Lang, W.; Colonna, P.; Almbauer, R. Assessment of Waste Heat Recovery From a Heavy-Duty Truck Engine by Means of an ORC Turbogenerator. *J. Eng. Gas Turbines Power* **2013**, *135*, 042313. [CrossRef]
31. Uusitalo, A.; Turunen-Saaresti, T.; Honkatukia, J.; Colonna, P.; Larjola, J. Siloxanes as Working Fluids for Mini-ORC Systems Based on High-Speed Turbogenerator Technology. *J. Eng. Gas Turbines Power ASME* **2013**, *135*, 042305. [CrossRef]
32. Bahamonde, S.; Pini, M.; De Servi, C.; Rubino, A.; Colonna, P. Method for the Preliminary Fluid Dynamic Design of High-Temperature Mini-Organic Rankine Cycle Turbines. *J. Eng. Gas Turbines Power ASME* **2017**, *139*, 082606. [CrossRef]
33. Jankowski, M.; Klonowicz, P.; Borsukiewicz, A. Multi-objective optimization of an ORC power plant using one-dimensional design of a radial-inflow turbine with backswept rotor blades. *Energy* **2021**, *237*, 121506. [CrossRef]
34. Hagen, B.A.L.; Agromayor, R.; Neksa, P. Equation-oriented methods for design optimization and performance analysis of radial inflow turbines. *Energy* **2021**, *237*, 121596. [CrossRef]
35. Wang, Y.; Wang, J.; Cheng, Z.; Sun, Q.; Zhao, P.; Dai, Y. Dynamic performance of an organic Rankine cycle system with a dynamic turbine model: A comparison study. *Appl. Therm. Eng.* **2020**, *181*, 115940. [CrossRef]
36. Erbaş, M.; Bıyıkoğlu, A. Design and multi-objective optimization of organic Rankine turbine. *Int. J. Hydrogen Energy* **2015**, *40*, 15343–15351. [CrossRef]
37. Uusitalo, A.; Turunen-Saaresti, T.; Honkatukia, J.; Dhanasegaran, R. Experimental study of small scale and high expansion ratio ORC for recovering high temperature waste heat. *Energy* **2020**, *208*, 118321. [CrossRef]
38. White, M.T.; Sayma, A.I. A generalised assessment of working fluids and radial turbines for non-recuperated subcritical organic Rankine cycles. *Energies* **2018**, *11*, 800. [CrossRef]
39. Persky, R.; Sauret, E. Assessment of turbine performance variability in response to power block design decisions for SF6 and CO2 solar thermal power plants. *Energy Convers. Manag.* **2018**, *169*, 255–265. [CrossRef]
40. Fiaschi, D.; Manfrida, G.; Maraschiello, F. Thermo-fluid dynamics preliminary design of turbo-expanders for ORC cycles. *Appl. Energy* **2012**, *97*, 601–608. [CrossRef]
41. Popp, T.; Weiß, A.P.; Heberle, F.; Winkler, J.; Scharf, R.; Weith, T.; Brüggemann, D. Experimental Characterization of an Adaptive Supersonic Micro Turbine for Waste Heat Recovery Applications. *Energies* **2021**, *15*, 25. [CrossRef]
42. Mounier, V.; Olmedo, L.E.; Schiffmann, J. Small scale radial inflow turbine performance and pre-design maps for Organic Rankine Cycles. *Energy* **2018**, *143*, 1072–1084. [CrossRef]
43. Clemente, S.; Micheli, D.; Reini, M.; Taccani, R. Bottoming organic Rankine cycle for a small scale gas turbine: A comparison of different solutions. *Appl. Energy* **2013**, *106*, 355–364. [CrossRef]
44. Da Lio, L.; Manente, G.; Lazzaretto, A. New efficiency charts for the optimum design of axial flow turbines for organic Rankine cycles. *Energy* **2014**, *77*, 447–459. [CrossRef]
45. Salah, S.I.; White, M.T.; Sayma, A.I. A comparison of axial turbine loss models for air, sCO_2 and ORC turbines across a range of scales. *Int. J. Thermofluids* **2022**, *15*, 100156. [CrossRef]
46. Ziółkowski, P.; Hyrzyński, R.; Lemański, M.; Kraszewski, B.; Bykuć, S.; Głuch, S.; Sowiżdżał, A.; Pająk, L.; Wachowicz-Pyzik, A.; Badur, J. Different design aspects of an Organic Rankine Cycle turbine for electricity production using a geothermal binary power plant. *Energy Convers. Manag.* **2021**, *246*, 114672. [CrossRef]
47. La Seta, A.; Meroni, A.; Andreasen, J.G.; Pierobon, L.; Persico, G.; Haglind, F. Combined turbine and cycle optimization for organic Rankine cycle power systems Part A: Turbine model. *Energies* **2016**, *9*, 313. [CrossRef]
48. Witanowski, L.; Klonowicz, P.; Lampart, P.; Suchocki, T.; Jedrzejewski, L.; Zaniewski, D.; Klimaszewski, P. Optimization of an axial turbine for a small scale ORC waste heat recovery system. *Energy* **2020**, *205*, 118059. [CrossRef]

49. Quan, Y.; Liu, J.; Zhang, C.; Wen, J.; Xu, G.; Dong, B. Aerodynamic design of an axial impulse turbine for the high-temperature organic Rankine cycle. *Appl. Therm. Eng.* **2020**, *167*, 114708. [CrossRef]
50. Da Lio, L.; Manente, G.; Lazzaretto, A. Predicting the optimum design of single stage axial expanders in ORC systems: Is there a single efficiency map for different working fluids? *Appl. Energy* **2016**, *167*, 44–58. [CrossRef]
51. Weiß, A.P.; Popp, T.; Zinn, G.; Preißinger, M.; Brüggemann, D. A micro-turbine-generator-construction-kit (MTG-c-kit) for small scale waste heat recovery ORC-Plants. *Energy* **2019**, *181*, 51–55. [CrossRef]
52. Weiß, A.P.; Novotný, V.; Popp, T.; Streit, P.; Špale, J.; Zinn, G.; Kolovratník, M. Customized ORC micro turbo-expanders—From 1D design to modular construction kit and prospects of additive manufacturing. *Energy* **2020**, *209*, 118407. [CrossRef]
53. Mikielewicz, J.; Piwowarski, M.; Kosowski, K. Design analysis of turbines for co-generating micro-power plant working in accordance with organic Rankine's cycle. *Pol. Marit. Res.* **2009**, *16*, 34–38. [CrossRef]
54. Klonowicz, P.; Witanowski, Ł; Suchocki, T.; Jędrzejewski, Ł; Lampart, P. Selection of optimum degree of partial admission in a laboratory organic vapour microturbine. *Energy Convers. Manag.* **2019**, *202*, 112189. [CrossRef]
55. Martins, G.L.; Braga, S.L.; Ferreira, S.B. Design optimization of partial admission axial turbine for ORC service. *Appl. Therm Eng.* **2016**, *96*, 18–25. [CrossRef]
56. Exergy Company. Exergy's Radial Outflow Turbine. Available online: https://www.exergy-orc.com/technology/radial-outflow-turbine/ (accessed on 20 March 2023).
57. Casati, E.; Vitale, S.; Pini, M.; Persico, G.; Colonna, P. Centrifugal Turbines for Mini-Organic Rankine Cycle Power Systems. *J. Eng. Gas Turbines Power ASME* **2014**, *136*, 122607. [CrossRef]
58. Kim, J.-S.; Kim, D.-Y. Preliminary Design and Off-Design Analysis of a Radial Outflow Turbine for Organic Rankine Cycles. *Energies* **2020**, *13*, 2118. [CrossRef]
59. Coronetta, U.; Sciubba, E. Optimal Design of a Ljungström Turbine for ORC Power Plants: From a 2D model to a 3D CFD Validation. *Int. J. Turbomachinery, Propuls. Power* **2020**, *5*, 19. [CrossRef]
60. Suhrmann, J.F.; Peitsch, D.; Gugau, M.; Heuer, T.; Tomm, U. Validation and development of loss models for small size radial turbines. In Proceedings of the ASME Turbo Expo 2010: Power for Land, Sea, and Air, Glasgow, UK, 14–18 June 2010; ASME: New York, NY, USA, 2010; pp. 1937–1949.
61. Alawadhi, K.; Alhouli, Y.; Ashour, A.; Alfalah, A. Design and Optimization of a Radial Turbine to Be Used in a Rankine Cycle Operating with an OTEC System. *J. Mar. Sci. Eng.* **2020**, *8*, 855. [CrossRef]
62. Rodgers, C. *Mainline Performance Prediction for Radial Inflow Turbines*; Lecture Series on Small High Pressure Ratio Turbines; Technical Report; Von Karman Institute for Fluid Dynamics: Brussels, Belgium, 1987.
63. Rohlik, H.E.; Kofskey, M.G. Recent radial turbine research at the NASA Lewis research center. In Proceedings of the ASME 1972 International Gas Turbine and Fluids Engineering Conference and Products Show, San Francisco, CA, USA, 26–30 March 1972; American Society of Mechanical Engineers: New York, NY, USA, 1972.
64. Glassman, A.J. *Enhanced Analysis and Users Manual for Radial-Inflow Turbine Conceptual Design Code*; RTD Technical Report; NASA: Washington, DC, USA, 1995.
65. Aungier, R.H. *Turbine Aerodynamics: Axial-Flow and Radial-Flow Turbine Design and Analysis*; ASME Press: New York, NY, USA, 2006.
66. Kastner, L.; Bhinder, F. A method for predicting the performance of a centripetal gas turbine fitted with a nozzle-less volute casing. In Proceedings of the ASME 1975 International Gas Turbine Conference and Products Show, Houston, TX, USA, 2–6 March 1975; American Society of Mechanical Engineers: New York, NY, USA, 1975.
67. Moustapha, H.; Zelesky, M.F.; Baines, N.C.; Japikse, D. *Axial and Radial Turbines*; Concepts NREC: White River Junction, VT, USA, 2003.
68. Daily, J.W.; Nece, R.E. Chamber dimension effects on induced flow and frictional resistance of enclosed rotating disks. *J. Basic Eng.* **1960**, *82*, 217–230. [CrossRef]
69. Whitfield, A.; Baines, N.C. *Design of Radial Turbomachines*, 1st ed.; Longman: New York, NY, USA, 1990.
70. Whitfield, A.; Wallace, F.J. Study of incidence loss models in radial and mixed-flow turbomachinery. In Proceedings of the IME—Conference on Heat and Fluid Flow in Steam and Gas Turbine Plant, Coventry, England, Coventry, UK, 3–5 April 1973.
71. Rodgers, C. Performance of High-Efficiency Radial/Axial Turbine. *J. Turbomach.* **1987**, *109*, 151–154. [CrossRef]
72. Runstadler, P.W.; Dolan, F.X.; Dean, R.C. *Diffuser Data Book*; CREARE Inc.: Hanover, NH, USA, 1974.
73. Dixon, S.L. *Fluid Mechanics and Thermodynamics of Turbomachinery*, 4th ed.; Butterworth-Heinemann: Oxford, UK, 1998.
74. Benson, R.S. A review of methods for assessing loss coefficients in radial gas turbines. *Int. J. Mech. Sci.* **1970**, *12*, 905–932. [CrossRef]
75. Whitfield, A. The preliminary design of radial inflow turbines. *ASME J. Turbomach.* **1990**, *112*, 51–57. [CrossRef]
76. Wasserbauer, C.A.; Glassman, A.J. *FORTRAN Program for Predicting the Off-Design Performance of Radial Inflow Turbines*; NASA: Washington, DC, USA, 1975; TN-8063.
77. Krylov, Y.P.; Spunde, Y.A. *About the Influence of the Clearance between the Working Blades and Housing of a Radial Turbine on Its Exponent*; FTD-MT-67-15; USAF Foreign Technology Division Translation: Dayton, OH, USA, 1963.
78. Dambach, R.; Hodson, H.P.; Huntsman, I. An experimental study of tip clearance flow in radial inflow turbine. In Proceedings of the ASME 1998 International Gas Turbine and Aeroengine Congress and Exhibition, Stockholm, Sweden, 2–5 June 1988. ASME Paper No. 98-GT-467.

79. Japikse, D.; Baines, N.C. *Introduction to Turbomachinery*, 1st ed.; Concepts ETI, Inc.; Oxford University Press: Oxford, UK, 1997.
80. Ghosh, S.K.; Sahoo, R.K.; Sarangi, S.K. Mathematical analysis for off-design performance of cyogenic turboexpander. *Trans. ASME J. Fluids Eng.* **2011**, *133*, 031001. [CrossRef]
81. Persky, R.; Sauret, E. Loss models for on and off-design performance of radial inflow turbomachinery. *Appl. Therm. Eng.* **2019**, *150*, 1066–1077. [CrossRef]
82. Wu, T.; Meng, X.; Wei, X.; Han, J.; Ma, X.; Han, J.; Shao, L. Design and performance analysis of a radial inflow turbogenerator with the aerostatic bearings for organic Rankine cycle system. *Energy Convers. Manag.* **2020**, *214*, 112910. [CrossRef]
83. Ainley, D.; Mathieson, G.C. *A Method of Performance Estimation for Axial-Flow Turbines*; Technical Report; Aeronautical Research Council: Khartoum, Sudan, 1951.
84. Dunham, J.; Came, P.M. Improvements to the Ainley-Mathieson method of turbine performance prediction. *J. Eng. Power* **1970**, *92*, 252–256. [CrossRef]
85. Kacker, S.C.; Okapuu, U. A mean line prediction method for axial flow turbine efficiency. *J. Eng. Power* **1982**, *104*, 111–119. [CrossRef]
86. Craig, H.R.M.; Cox, H.J.A. Performance estimation of axial flow turbines. *Proc. Inst. Mech. Eng.* **1970**, *185*, 407–424. [CrossRef]
87. Klonowicz, P.; Heberle, F.; Preißinger, M.; Brüggemann, D. Significance of loss correlations in performance prediction of small scale, highly loaded turbine stages working in Organic Rankine Cycles. *Energy* **2014**, *72*, 322–330. [CrossRef]
88. Peng, N.; Wang, E.; Meng, F. Off-design performance comparison of single-stage axial turbines using CO2 and zeotropic mixture for low-temperature heat source. *Energy Convers. Manag.* **2020**, *213*, 112838. [CrossRef]
89. Peng, N.; Wang, E.; Zhang, H. Preliminary Design of an Axial-Flow Turbine for Small-Scale Supercritical Organic Rankine Cycle. *Energies* **2021**, *14*, 5277. [CrossRef]
90. Peng, N.; Wang, E.; Wang, W. Design and analysis of a 1.5 kW single-stage partial-admission impulse turbine for low-grade energy utilization. *Energy* **2023**, *268*, 126631. [CrossRef]
91. Wei, N. *Significance of Loss Models in Aerothermodynamic Simulation for Axial Turbines*; Royal Institute of Technology: Stockholm, Sweden, 2000.
92. Schittkowski, K. NLPQL: A FORTRAN subroutine solving constrained nonlinear programming problems. *Ann. Oper. Res.* **1985**, *5*, 485–500. [CrossRef]
93. Han, Z.; Jia, X.; Li, P. Improved thermodynamic and aerodynamic design method and off-design performance analysis of a radial inflow turbine for ORC system. *Int. J. Energy Res.* **2019**, *43*, 8337–8349. [CrossRef]
94. Zhai, L.; Xu, G.; Wen, J.; Quan, Y.; Fu, J.; Wu, H.; Li, T. An improved modeling for low-grade organic Rankine cycle coupled with optimization design of radial-inflow turbine. *Energy Convers. Manag.* **2017**, *153*, 60–70. [CrossRef]
95. Li, W.; Ling, X. An optimization framework development for organic rankine cycle driven by waste heat recovery: Based on the radial-inflow turbine. *Case Stud. Therm. Eng.* **2022**, *34*, 102054. [CrossRef]
96. Li, Y.; Li, W.; Gao, X.; Ling, X. Thermodynamic analysis and optimization of organic Rankine cycles based on radial-inflow turbine design. *Appl. Therm. Eng.* **2021**, *184*, 116277. [CrossRef]
97. Björkman, M.; Holmström, K. Global optimization using the DIRECT algorithm in matlab. *Adv. Model. Optim.* **1999**, *1*, 17–37.